Evaluation of enzymatic browning in fresh-cut apple slices applying a multispectral vision system

PRESENTED BY DIEZMA BELEN

L. Lunadei [a], P. Galleguillos [b], B. Diezma [a], L. Lleó [c]

[a] Laboratorio de Propiedades Físicas y Tecnologías Avanzadas en Agroalimentación, Departamento de Ingeniería Rural, E.T.S.I. Agrónomos, Universidad Politécnica de Madrid, Av. Complutense s/n, Ciudad Universitaria, 28040 Madrid, Spain. loredana.lunadei@upm.es
[b] Grupo de Estudios Postcosecha, Departamento de Producción Agrícola, Facultad de Ciencias Agronómicas, Universidad de Chile, c/ Santa Rosa 11315, Santiago de Chile, Chile.
[c] Departamento de Ciencia y Tecnologías Aplicadas a la Ingeniería Técnica Agrícola, E.U.I.T. Agrónomos, Universidad Politécnica de Madrid, Av. Complutense s/n, Ciudad Universitaria, 28040 Madrid, Spain.

Abstract

In this study a vision system was applied for assessing enzymatic browning evolution in fresh-cut apples slices stored at 7.5 °C and 85 % HR. Twenty-four slices were analyzed per day: at zero time and after storage for 1, 3, 7 and 9 days. A classification procedure was applied to virtual images obtained as a combination of the red (R) and blue (B) channel (B/R, R–B and R-B/R+B). In all cases, three images based browning reference classes were generated. An external validation was applied to a second set of samples submitted to the same treatments, obtaining a high percentage of samples correctly classified. Camera classification was evaluated according to colorimetric measurements usually utilized to evaluate enzymatic browning: CIE L*a*b* colour parameters and browning index (BI). Virtual image based on B/R showed the best sensitivity to reflect the change in colours associated with browning.

Key words: *fresh-cut apples; enzymatic browning; image analysis.*

1. Introduction

Fresh-cut apples have recently emerged as a popular snack in food service establishments, school lunch programs and for family consumption. The market for fresh-cut apples is projected to continue to grow as more consumers demand fresh, convenient and nutritious snacks (Lu et al. 2007). However, the act of cutting fresh products invariably enhances degradative changes, which present additional challenges to the industry to maintain quality for an acceptable marketing period. An important factor causing loss of quality in much products is the development of browning in cut surface (Pristijono et al. 2006).

Traditionally, enzymatic browning has been quantified using browning indicators through a biochemical index, for example using polyphenol oxidase activity (Osanai et al. 2003; Hosoda et al. 2005) or physical indicators, such as colour surface (Kang et al. 2004; Lu 2004). In the case of physical indicators based on colour, CIE *L*a*b** colour space has been the most extensively used colour reference, due to the uniform distribution of colours and because it is very close to human perception of colour (Yam et al. 2004). Based on CIE *L*a*b** coordinates, especially on the *L** value, or on CIE *XYZ* colour space (strongly related to the *Lab*), browning indicators in fruits have been developed (Valentines et al. 2005; Lu et al. 2007). Browning index (BI), defined as brown colour purity, is one of the most common indicators of browning in sugar containing food products (Buera et al. 1986). In order to carry out a detailed characterization of the colour of a food item and thus more precisely evaluated its quality, it is necessary to know the colour value of each point of its surface. However, at

present available commercial colorimeters measure $L^*a^*b^*$ coordinates only over a very few square centimetres, and thus their measurements could be not very representative in heterogeneous materials such as most food products (Papadakis et al. 2000). Furthermore, the global analysis of the foods surface becomes more difficult (Mendoza et al. 2004).Recently, Leon et al. (2006) have suggested a computer vision system (CVS) to measure colour in $L^*a^*b^*$ coordinates from RGB space to be used in image analysis and some studies have been undertaken applying that approximation to food (Pedreschi et al. 2007; Quevedo et al. 2008). During the description of browning kinetics using colour information, an average of the L^* values is usually calculated for colorimeter devices using a CVS for an analyzed area. However, in apple slices, the development of non-uniform colour patterns during browning (specifically for L^*), is observed. An approximation aimed at quantifying non-homogenous colour surfaces in apple slices during enzymatic browning was undertaken by Yoruk et al. (2004); nevertheless, due to the complexity of analyzing and displaying the frequency of 16.7 million colours, they adopted a sub-colour space deriving from the RGB one, in which each colour axis (Red, Green, Blue), which normally ranges from 0 to 255 was, was divided into eight and the colours were so regrouped in 8 x 8 x 8 = 512 ranges. Texture image analysis has been suggested as one tool to quantify colour information extracted from both grey and colour images, without reducing the intensity levels of RGB components. This has been possible because texture of images is usually determinate by analyzing the surface intensity obtained by plotting the (x, y) pixel coordinates versus the gray level of each pixel (z axis): the changes in pixel value intensity reflect the texture of the image, which might contain information about the colour and the geometric structure of objects (Quevedo et al. 2002; Du et al. 2004; Zheng et al. 2006; Gonzales-Barron et al. 2008). However, up to now image texture analysis has been employed to quantify the non-homogenous distribution of the L^* coordinate in fresh-cut products with a cubical shape (Quevedo et al. 2009a; Quevedo et al. 2009b; Quevedo et al. 2009c).

Spectral considerations about plant pigments content evaluation

When assessing enzymatic browning with a vision system, it is important to identify spectral changes associated with pigments evolution during the browning process. After performing colorimetric analysis based on CIE $L^*a^*b^*$ colour space, several authors have observed that an increase in enzymatic browning in apple pieces during storage is accompanied by an increase in colorimetric a^* and b^* values, and a decrease in lightness (L^*) and hue values (Sims et al. 2002; Pristijono et al. 2006; Lu et al. 2007). L^* is the luminance component (it ranges from 0 to 100), while a^* and b^* are colour coordinates related respectively with the red/green and yellow/blue spectral ranges, with values varying from -120 to +120 (Yam and Papadakis 2004). The decrease of the L^* values means that during the browning apple surface turns darker, while its colour turn to red and yellow, due to an increase in a^* and b^* colour coordinates. Fig. 1 presents the shape of a reflectance spectrum of a fresh-cut apple slice at zero time (t_0) and of the same sample after 9 days (t_9) stored ad 7.5 ºC. The main differences are that relative reflectance values in the green and blue (430-490 nm approximately) areas are higher at the beginning of the storage period than at the end. On the contrary, reflectance values in the yellow and red (620-700 nm approximately) ranges are lower at t_0 than at t_9.

Aims and objectives of the research

The objective of the present research was to develop a multispectral vision system in order to classify fresh-cut apple slices according to their browning evolution. The aim was to identify the best virtual image (obtained as a combination of monochromatic images) able to detect changes in colour related with this physiological process.

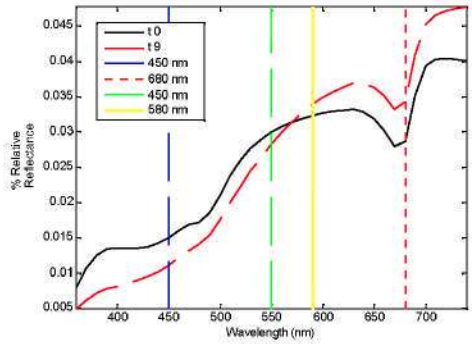

Fig. 1: VIS relative reflectance spectra belonging to a fresh-cut apple slice at zero time (t_0) and to the same sample stored ad 7.5 °C during 9 days (t_9).

2. Materials and methods

Fruit samples

Fifteen apples var. *Granny Smith* were peeled and cut into eight equal slices, obtaining a total of 120 slices (*set 1*). Single slice were considered as sample units in this work. Fruit slices were stored at 7.5 °C and 85 % HR, covered with a cling film. Twenty-four samples were evaluated at zero time and after storage for 1, 3, 7 and 9 days. In this work each storage time corresponds to a treatment. A second set (*set 2*) of 120 samples was prepared in the same way and submitted to the same treatments that *set 1*.

Reference values

Non-destructive (ND) reference tests were carried out on both *set 1* and *set 2* samples through a portable spectrophotometer Minolta CM-50I (Konica Minolta Sensing, Inc., Japan). A standard white calibration plate was employed to calibrate the equipment. Measurements were performed on one side of each apple slice, in three different points of the cut area.

Reflectance spectra analysis

Visible relative reflectance spectra 360-740 nm, at 10 nm intervals, were obtained for each sample. A forward stepwise discriminant analysis was performed to the reflectance data, in order to reduce the original number of variables (λ), corresponding to the wavelengths (360-740 nm), to a subset of dependent variables (λ_p), where it was possible to observe the main differences between the spectra, coinciding with the optimal optical range to detect browning. Five levels in the categorical variable were used, corresponding to the five treatments (t_0, t_1, t_3, t_7 and t_9).

Colour parameters

CIE *L*a*b** coordinates were measured and the results were also reported as *XYZ* tristimulus values. In this way it was possible to calculate the browning index (BI), by applying the equation [1]:

$$BI = \frac{(x - 0.31)}{0.172} \times 100 \qquad [1]$$

Where x is the chromaticity coordinate calculated from the XYZ values, according to the following formula $x = X/(X+Y+Z)$. ANOVA analysis was applied to the BI values and to each treatment. The results were employed as a reference of browning evolution during storage with regard to multispectral image information. All analysis were carried out using MATLAB® (MathWorks, Inc., USA).

Vision system

Images were acquired through a multispectral image system consisting of a frame-grabber and a 3 CCD camera (DuncanTech/Redlake MS-3100®, Redlake Inc., USA) with digital output. Camera resolution was 1300×1000 pixels, endowed with three band-pass filters (band-width: 20 nm), centred at 800 nm (infrared, IR), 680 nm (red, R), and 450 nm (blue, B) and three monochromatic images can be analyzed from each sample: IR, R and B. The light source was provided by six 100W/220V halogen lamps and the object distance between the lens system and the sample was 60 cm. The angle between the camera lens axis and the lighting source axis was 45º. The images were acquired using a black background. A black canvas was put around the vision test station, in order to create a uniform light field around the object and to eliminate any effect of environmental light.

Image analysis: image segmentation and virtual images calculation

An image was acquired for each sample. At first, apple slice samples were distinguished from the background through the *Otsu method* (Otsu 1979), a segmentation technique very commonly used in the bibliography. This technique computes threshold level on the basis of the image histogram distribution. It was performed on the R images, since they presented the greatest difference between the gray levels corresponding to samples (the region of interest) and to background. This operation results in a binary image which could be considered as an "image mask", in which only the pixels representing the sample were white, while the pixels corresponding to the background were black. This image mask was multiplied for the different type of images performed in this research.

On the basis of the main differences found between spectra from samples with and without browning (Fig. 1), two wavelengths, and its corresponding channels, has been selected in order to generate virtual images: R (680 nm) and B (450 nm) channels. The following combinations of these channels were tested: B/R (B image divided by R image pixel by pixel), R–B (difference between the R and the B images) and R-B/R+B. Further analysis were based on the relative histograms of the described virtual images, computed as relative frequency of pixels over the intensity range of the image. In the present work, index 1 (Ind_1), index 2 (Ind_2) and index 3 (Ind_3) were employed to refer respectively to the R-B/R+B, R–B and B/R combination of monochromatic images and in what follow, "histogram" refers to "relative histogram" of the image.

Non-supervised image classification

A non-supervised classification according to Ward's method was performed in order to define *browning reference classes* (BRC) based on *set 1* histograms calculated from Ind_1, Ind_2 and Ind_3 images. All the intensity levels of the histograms were considered as the dimensions of a multidimensional space, where a single histogram was represented as a single point. The matrix of Euclidean distances between each pair of individuals (histograms) was computed in order to group the closest ones and to hierarchically merge individuals whose combination gave the least *Ward Linkage distance* (that is the minimum increase within sum of squares of the new-formed group).

As an advantage to other classification methods, Ward's method takes into account all histograms of the data set at every level of the grouping, producing very well structured and homogeneous groups. Besides, this method allowed successful results in precedent works investigating fruit ripeness (Herrero A. et al. 2010 (*in press*)). A MATLAB® devoted code was developed in order to generate automatically the groups on the basis of an input maximum *Ward linkage distance*, derived from the analysis of the cluster tree features. The average histogram was computed for each generated group and defined as BRC.

Validation: classification of anonymous samples into browning reference classes

External validation was carried out by assigning each anonymous individual into the previously generated BRC (each one defined by the average histogram of the class) to which it computed the minimum *Euclidean distance* (E_d). In order to test the robustness of the model based on *set 1* data, an external validation procedure was performed: the *observed* classification of *set 2* samples was compared with the *predicted* classification of each anonymous histogram through the minimum E_d to the BRC generated with the *set 1* population.

Statistical analysis

The colour reference parameters (BI and CIE *L*a*b** coordinates) were compared to the classification based on the histograms of virtual images of each index. ANOVA analysis was applied to the BI and CIE *L*a*b** values and to the classes extracted from the image analysis.

3. Results

Reflectance spectra discriminant analysis

The stepwise method operated in a iterative manner, adding the variables whose F-statistics were greater than the F_{in} value. To eliminate the variables that provided superfluous information at a 99% confidence level, a F_{in} = 6.87 with tolerance of 0.01 was applied in the forward stepwise procedure. Iteratively, the algorithm took various steps to converge, producing a subset containing the most significant wavelengths to identify browning. The selected subset was formed by wavelengths belonging to the red range, *i.e.*, 620, 650, 660, 670 and 680 nm, and to the blue range, *i.e.*, 430, 470 and 490 nm. This subset of wavelengths let to discriminate correctly a high percentage of samples (92-100 %) on the basis of their treatment. Besides, the samples that were incorrectly classified (0-8 %) were assigned to the immediately previous (or following) class. This means that in almost all cases the wavelengths corresponding to the red, whose reflectance values increase, and to the blue range, in which relative reflectance decreases, were able to identify spectral changes associated with pigment evolution related with the browning process.

Generation of browning reference classes

First column of Fig. 2 shows the average histograms calculated for each treatment and for each image combination. How the above consideration suggested, the average histograms calculated from Ind_1 and Ind_2 shifted to higher intensity values, while images based on Ind_3 moved to lower ones. Fig. 2 also reports the dendrograms generated by applying Ward's non supervised classification to each image combination. On the basis of the dendrogram features, the maximum *Ward Linkage distance* within groups was set at 0.30 pixel relative frequency. In all cases, three clusters, corresponding to three BRC (Class A, Class B and Class C) were obtained. In the same figure the average histograms corresponding to these three clusters are also showed.

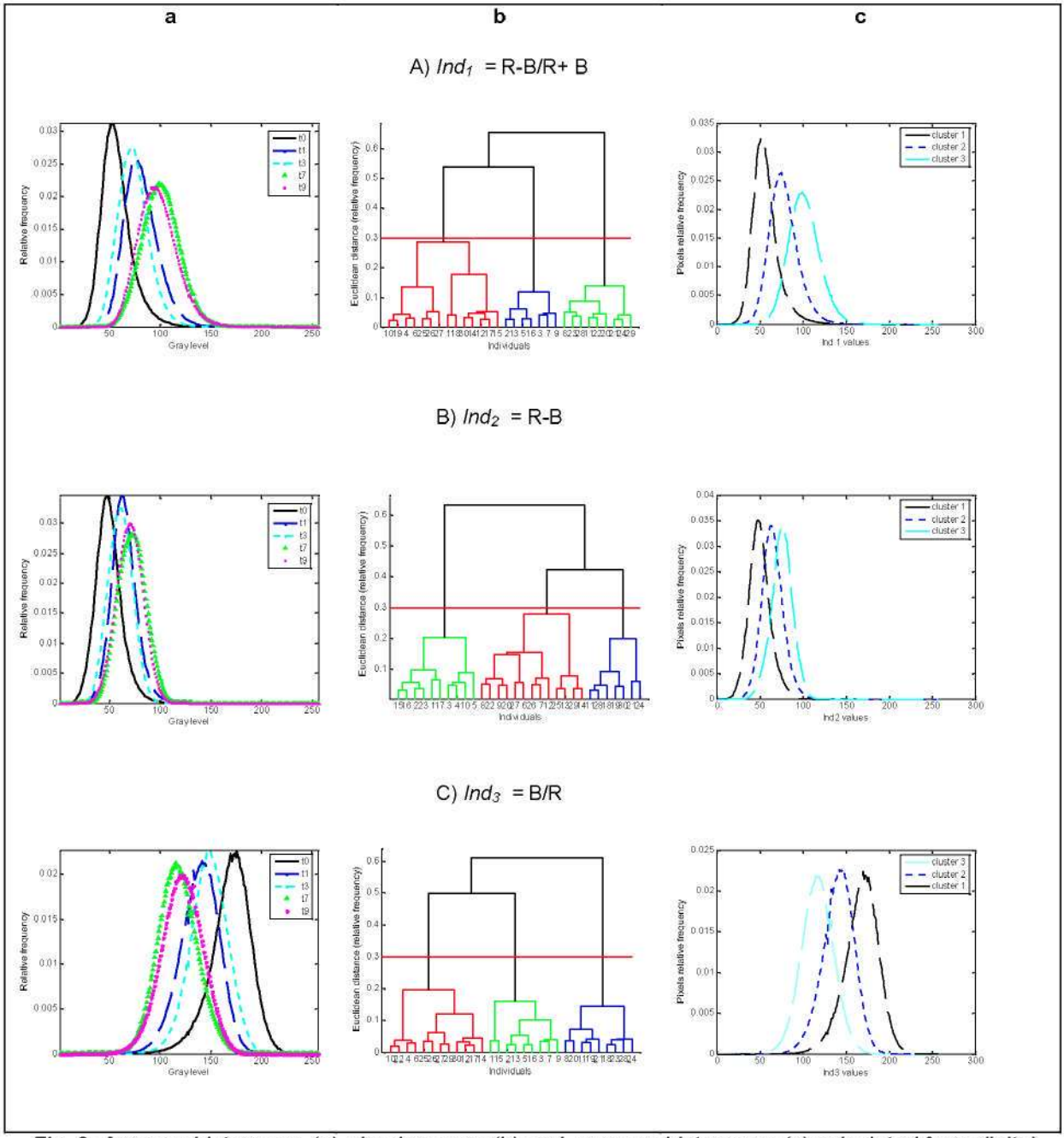

Fig. 2: Average histograms (a), dendrograms (b) and average histograms (c) calculated from digital images of the set 1 samples based on Ind_1 (panel A), Ind_2 (panel B) and Ind_3 (panel C).

Table 1 reports, for each image combination, the classification matrix obtained by applying the Ward's non-supervised classification. For the three image indexes, Class A was mainly composed by samples measured at zero time, respectively 95, 76 and 84 %, Class B included 78, 60 and 81 % of samples measured after one and three days of storage, while Class C comprised 93, 92 and 93 % of the samples measured on the 7th and the 9th day. Therefore the three non-supervised classifications based on the virtual images were able to segregate storage periods, differentiating samples analyzed on the first day from samples analyzed on the second-third day and on the last two days of storage.

Tab. 1: Classification matrix of set 1 samples: treatments (observed classification) against reference camera classification (predicted classification).

		OBSERVED		
	Classes \ Treatments	t_0	t_1-t_3	t_7-t_9
		Ind $_1$= R-B/R+B		
PREDICTED	**A**	21	1	
	B	3	44	9
	C		3	39
		Ind $_2$= R-B		
	A	22	6	1
	B	2	40	26
	C		2	22
		Ind $_3$= B/R		
	A	24	6	
	B		39	9
	C		3	39

Fig. 3 plots the average values and confidence intervals (95%) of BI and CIE *L*a*b** coordinates for each image based class. ANOVA results performed on colour parameters showed that BI, *a** and *b** values presented a consistent increase from Class A to C, while L* decreased from Class A to C. These results are according to previous works that studied colour coordinates evolution related to enzymatic browning during storage (Perez-Gago et al. 2006; Lu et al. 2007).The best accordance between the image-based classes and their reference values was shown by *a** and BI values. According to *L** parameter, class A and B are not significantly different and could be grouped in the same class. Pristijono at al. (2006) in a research regarding browning inhibitory techniques in Granny Smith apple slices, an *L** value of 76.0 was considered as a limit of acceptability of browning and Class C was thus considered the class of samples exhibiting severe browning. Considering the Fisher Least Significant Differences (LSD) test, the classification based on Ind_3 showed the best accordance with the colour parameters, succeeded by Ind_1 and Ind_2 (table not shown). On the basis of these results, image based classes may provide relevant information for the management of fresh-cut apple slices, showing good potential to select fruits with an unacceptable level of browning.

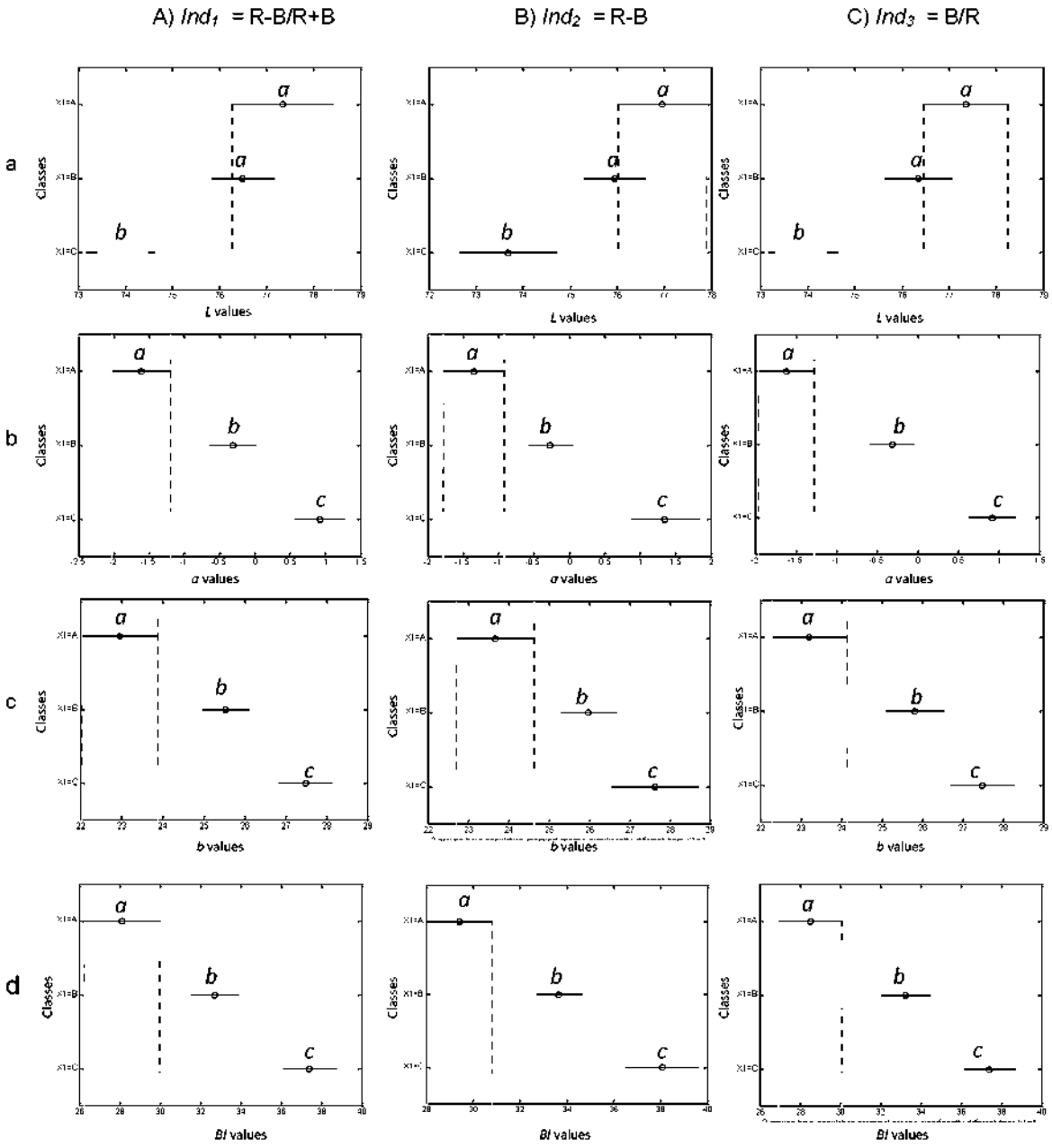

*Fig. 3: From figures **a** to **d**: Plot of averages and confidence intervals (95%) of L*, a*, b* and BI values (x axis) of set 1 samples, classified in classes A to C (y axis) according to Ward's method based on Ind_1 (column A), Ind_2 (column B) and Ind_3 (column C) image histograms. Means characterized by the same letter are not significantly different by ANOVA Fisher Least Significant Differences (LSD) test ($p<0.05$); different letters implies there is significant difference between means.*

From ANOVA analysis applied to the BI values for each treatment resulted that the confidence intervals (95%) of the all samples corresponding to the t_9 treatment ranged from BI_{min} = 36 to BI_{max} = 40 (data not shown). From this result BI = 36 was proposed as threshold value for browning detection (BI_{limit}). Fig. 4 displays BI values for each *set 1* sample categorized in their corresponding image based class for the three image combinations. Considering camera classification, almost all the samples of Class A (97 % in the case of Ind_2 and Ind_3 and 95 % for Ind_1) and between 86 % (Ind_1) and 83 % (Ind_2 and Ind_3) of the samples assigned to Class B were characterized by a BI value lower than BI_{limit}.

Class C was constituted by 46 % (Ind_2) and 43 % (Ind_1 and Ind_3) of samples with BI value higher than the BI threshold. These results confirmed that Class A and B would be mainly constituted by samples with a cut surface without or with a moderate browning, while half of samples of Class C would exhibit a severe browning.

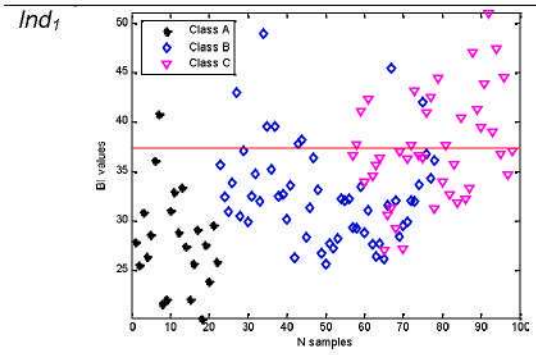

	N samples	<BI$_{limit}$	
		n	%
Class A	22	21	95
Class B	56	48	86
Class C	42	24	57

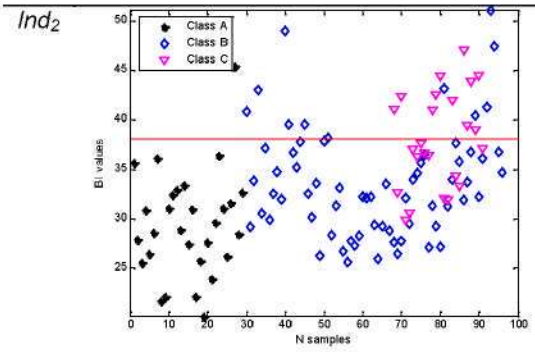

	N samples	<BI$_{limit}$	
		n	%
Class A	29	28	97
Class B	67	56	83
Class C	24	13	54

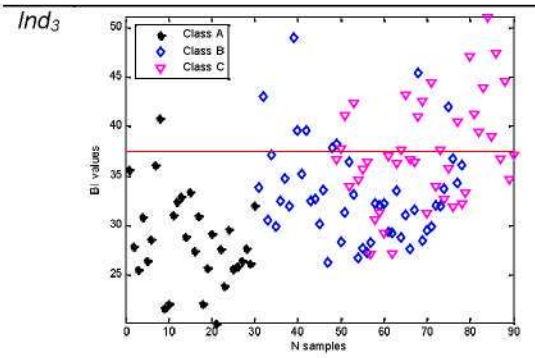

	N samples	<BI$_{limit}$	
		n	%
Class A	30	29	97
Class B	48	40	83
Class C	42	24	57

Fig. 4: On the left: BI values of set 1 samples categorized in their corresponding image based class (A, B and C) for the three image combinations. Horizontal lines represent BI$_{limit}$. On the right: number of set 1 samples assigned to each image based class categorized in their corresponding BI range.

External validation

The proposed classification procedure, obtained through the minimum distance to the reference classes generated with Ind_1, Ind_2 and Ind_3 histograms of *set 1* samples, was able to classify correctly, respectively, 95, 92 and 75 from the 120 samples considered from *set 2*. According to the aforementioned BI$_{limit}$ value, between 81 % (Ind_3) and 95 % (Ind_1) of the samples assigned to Class A and between 68 % (Ind_2) and 95 % (Ind_3) of those assigned to Class B would be below the threshold BI value.

4. Conclusion

In the present work a new method to classify fresh-cut apple slices on the basis of enzymatic browning evolution applying a multispectral vision system was presented. The method utilized relative histograms of virtual images, *e.g.*, Ind_1, Ind_2 and Ind_3 indexes, combinations of red (R, 680 nm) and blue (B, 450 nm) images of the samples. Red and blue spectral ranges turn out to contain enough information for the proposed method to adequately classify samples images. On the basis of internal classification results, all the indexes were able to detect browning evolution, classifying samples into three reference classes (A to C). In all cases, Class A to C presented decreasing lightness and increasing BI, a^* and b^* values. Image combination based on Ind_3 showed the best sensitivity to reflect the change in colours associated with browning. The robustness of the model and classification procedure was observed applying an external validation to a second set of samples. It was possible to classify images from fruits of second testing set with the model generated with the first set, obtaining similar average and range of colour coordinates for the image-based classes. All these results present the potential of the proposed method to characterize enzymatic browning evolution in fresh-cut apples. It could be used as a potential criterion for establishing the optimal shelf-life of fresh-cut apple slices under refrigeration condition. Besides, this method allows a spatially detailed determination compared to colorimetric techniques that give a global determination of the browning stage.

References

Buera, M. P., Lozano, R. D., & Petriella, C. (1986). Definition of colour in the non enzymatic browning process. *Die. Farbe*, 32, 318-322.

Du, C.-J., & Sun, D.-W. (2004). Recent developments in the applications of image processing techniques for food quality evaluation. *Trends in Food Science & Technology*, 15 (5), 230-249.

Gonzales-Barron, U., & Butler, F. (2008). Discrimination of crumb grain visual appearance of organic and non-organic bread loaves by image texture analysis. *Journal of Food Engineering*, 84 (3), 480-488.

Herrero A., Lunadei L., Lleó L., Diezma B., & M., R. (2010 (*in press*)). Multispectral Vision for Monitoring Fruit Ripeness. *journal of Food Scince*.

Hosoda, H., Inoue, E., Iwahashi, Y., Sakaue, K., Tada, M., & Nagata, T. (2005). Inhibitory effect of sulfides on browning of apple slice. *Journal of the Japanese Society for Food Science and Technology*, 52, 120-124.

Kang, K. J., Oh, G. S., Go, Y. S., Kim, Y. J., Park, D. H., & Kim, H. Y. (2004). Inhibition of enzymatic browning in Paeoniae radix rubra by citric acid. *Food Science and Biotechnology Advances*, 13, 119-125.

León, K., Mery, D., Pedreschi, F., & León, J. (2006). Color measurement in L*a*b* units from RGB digital images. *Food Research International*, 39 (10), 1084-1091.

Lu, R. (2004). Multispectral imaging for predicting firmness and soluble solids content of apple fruit. *Postharvest Biology and Technology*, 31 (2), 147-157.

Lu, S., Luo, Y., Turner, E., & Feng, H. (2007). Efficacy of sodium chlorite as an inhibitor of enzymatic browning in apple slices. *Food Chemistry*, 104 (2), 824-829.

Mendoza, F., & Aguilera, J. M. (2004). Application of Image Analysis for Classification of Ripening Bananas. *Journal of Food Science*, 69 (9), E471 - E477.

Osanai, Y., Motomura, Y., & Sakurai, N. (2003). Effect of methyl bromide on the internal browning, firmness and elasticity of flesh in un-bagged apple 'Fuji' fruit. *Journal of the Japanese Society for Food Science and Technology* (50), 254-258.

Otsu, N. (1979). A threshold selection method from gray-level histograms. *IEEE Transactions on System Man & Cybernetics*, 9, 62-66.

Papadakis, S. E., Malek, S. A., Emery, R. E., & Yam, K. L. (2000). A Versatile and Inexpensive Technique for Measuring Color of Foods. *Food Technology*, 54, 48-51.
Pedreschi, F., Bustos, O., Mery, D., Moyano, P., Kaack, K., & Granby, K. (2007). Color kinetics and acrylamide formation in NaCl soaked potato chips. *Journal of Food Engineering*, 79 (3), 989-997.
Perez-Gago, M. B., Serra, M., & Río, M. A. d. (2006). Color change of fresh-cut apples coated with whey protein concentrate-based edible coatings. *Postharvest Biology and Technology*, 39 (1), 84-92.
Pristijono, P., Wills, R. B. H., & Golding, J. B. (2006). Inhibition of browning on the surface of apple slices by short term exposure to nitric oxide (NO) gas. *Postharvest Biology and Technology*, 42 (3), 256-259.
Quevedo, R., Aguilera, J. M., & Pedreschi, F. (2008). Color of salmon fillets by computer vision and sensory panel. *Food and Bioprocess Technology*, doi:10.1007/s11947-008-0106-6.
Quevedo, R., Carlos, L.-G., Aguilera, J. M., & Cadoche, L. (2002). Description of food surfaces and microstructural changes using fractal image texture analysis. *Journal of Food Engineering*, 53 (4), 361-371.
Quevedo, R., Díaz, O., Caqueo, A., Ronceros, B., & Aguilera, J. M. (2009a). Quantification of enzymatic browning kinetics in pear slices using non-homogenous L* color information from digital images. *Food Science and Technology*, 42 (8), 1367-1373.
Quevedo, R., Díaz, O., Ronceros, B., Pedreschi, F., & Aguilera, J. M. (2009b). Description of the kinetic enzymatic browning in banana (Musa cavendish) slices using non-uniform color information from digital images. *Food Research International*, 42 (9), 1309-1314.
Quevedo, R., Jaramillo, M., Díaz, O., Pedreschi, F., & Aguilera, J. M. (2009c). Quantification of enzymatic browning in apple slices applying the fractal texture Fourier image. *Journal of Food Engineering*, 95 (2), 285-290.
Sims, D. A., & Gamon, J. A. (2002). Relationships between leaf pigment content and spectral reflectance across a wide range of species, leaf structures and developmental stages. *Remote Sensing of Environment*, 81 (2-3), 337-354.
Valentines, M. C., Vilaplana, R., Torres, R., Usall, J., & Larrigaudière, C. (2005). Specific roles of enzymatic browning and lignification in apple disease resistance. *Postharvest Biology and Technology*, 36 (3), 227-234.
Yam, K. L., & Papadakis, S. E. (2004). A simple digital imaging method for measuring and analyzing color of food surfaces. *Journal of Food Engineering*, 61 (1), 137-142.
Yoruk, R., Yoruk, S., Balaban, M. O., & Marshall, M. R. (2004). Machine vision analysis of antibrowning potency for oxalic acid: A comparative investigation on banana and apple. *Journal of Food Science and Technology (Mysore)*, 69, E281-E289.
Zheng, C., Sun, D.-W., & Zheng, L. (2006). Recent applications of image texture for evaluation of food qualities--a review. *Trends in Food Science & Technology*, 17 (3), 113-128.